

SANDIA REPORT

SAND2022-12375

Printed September, 2022



Sandia
National
Laboratories

Simulink Modeling and Dynamic Study of Fixed-Speed, Variable-Speed, and Ternary Pumped Storage Hydropower

Miguel Jimenez-Aparicio, Felipe Wilches-Bernal, Rachid Darbali-Zamora, Thad Haines, David A. Schoenwald, S. M. Shafiul Alam, Vahan Gevorgian, Weihang Yan

Prepared by
Sandia National Laboratories
Albuquerque, New Mexico 87185
Livermore, California 94550

Issued by Sandia National Laboratories, operated for the United States Department of Energy by National Technology & Engineering Solutions of Sandia, LLC.

NOTICE: This report was prepared as an account of work sponsored by an agency of the United States Government. Neither the United States Government, nor any agency thereof, nor any of their employees, nor any of their contractors, subcontractors, or their employees, make any warranty, express or implied, or assume any legal liability or responsibility for the accuracy, completeness, or usefulness of any information, apparatus, product, or process disclosed, or represent that its use would not infringe privately owned rights. Reference herein to any specific commercial product, process, or service by trade name, trademark, manufacturer, or otherwise, does not necessarily constitute or imply its endorsement, recommendation, or favoring by the United States Government, any agency thereof, or any of their contractors or subcontractors. The views and opinions expressed herein do not necessarily state or reflect those of the United States Government, any agency thereof, or any of their contractors.

Printed in the United States of America. This report has been reproduced directly from the best available copy.

Available to DOE and DOE contractors from

U.S. Department of Energy
Office of Scientific and Technical Information
P.O. Box 62
Oak Ridge, TN 37831

Telephone: (865) 576-8401
Facsimile: (865) 576-5728
E-Mail: reports@osti.gov
Online ordering: <http://www.osti.gov/scitech>

Available to the public from

U.S. Department of Commerce
National Technical Information Service
5301 Shawnee Road
Alexandria, VA 22312

Telephone: (800) 553-6847
Facsimile: (703) 605-6900
E-Mail: orders@ntis.gov
Online order: <https://classic.ntis.gov/help/order-methods>



Simulink Modeling and Dynamic Study of Fixed-Speed, Variable-Speed, and Ternary Pumped Storage Hydropower

Miguel Jimenez-Aparicio^{1*}, Felipe Wilches-Bernal¹, Rachid Darbali-Zamora¹, Thad Haines¹,
David A. Schoenwald¹, S. M. Shafiul Alam², Vahan Gevorgian³, Weihang Yan³

¹Sandia National Laboratories, Albuquerque, NM 87185, USA

²Idaho National Laboratory, Idaho Falls, ID 83415, USA

³National Renewable Energy Laboratory, Golden, CO 80401, USA

ABSTRACT

Pumped Storage Hydropower (PSH) is one of the most popular energy storage technologies in the world. It uses an upper reservoir to store water which can be later used during high-demand. In the United States, most of the energy storage capability actually corresponds to PSH. Moreover, PSH also brings multiple benefits to grid operation.

This report presents the Simulink models of three common PSH technologies: Fixed-Speed (FS), Variable-Speed (VS), and Ternary (T)-PSH. These models are available to the general public on this GitHub repository¹, which contains the MATLAB model initialization files, the Simulink model files, and supplementary MATLAB code used to obtain the figures in this work.

For each PSH model, an introductory description of the model components and other relevant functionalities are provided. For further information regarding the models and the initialization parameters, the reader is referred to the shared files in the repository. This report also presents the dynamic behavior of each model. The response of such models to a load event is analyzed and matched with each model's features. A custom IEEE 39 bus case is employed for the FS and T-PSH simulations, while the VS-PSH is simulated on a simplified three-bus test system due to the computational complexity of the model. For the T-PSH, the steady-state and the switching between several operating modes are also studied in this work.

SAND2022-12375

*Send correspondence to mjimene@sandia.gov.

¹See: https://github.com/sandialabs/Simulink_PumpedStorageHydropower.

ACKNOWLEDGMENT

This research was supported by the US Department of Energy (DOE) Water Power Technologies Office (WPTO) under the Grid Modernization Laboratory Consortium (GMLC) program.

Thanks to the entire FlexPower team for their collaboration during the development of the models.

CONTENTS

1. Introduction	9
2. Fixed-Speed PSH	10
2.1. Model description	10
2.2. Simulation: Load event for the FS-PSH in generating mode	11
2.3. Simulation: Load event for the FS-PSH in pumping mode	12
3. Variable-Speed PSH	14
3.1. Model description	14
3.2. Simulation: Load event for the VS-PSH during generating mode	16
3.3. Simulation: Load event for the VS-PSH during pumping mode	18
4. Ternary-PSH	21
4.1. Model description	21
4.2. Simulation: Steady-state	23
4.3. Simulation: Load Event	23
4.4. Simulation: Mode switching	30
5. Conclusions	33
Bibliography	34

LIST OF FIGURES

Figure 2-1.	FS-PSH diagram	11
Figure 2-2.	FS-PSH location in the IEEE 39 bus system	11
Figure 2-3.	FS-PSH response to load event during generating mode	12
Figure 2-4.	FS-PSH response to load event during pumping mode	13
Figure 3-1.	VS-PSH system diagram	15
Figure 3-2.	VS-PSH location in the simplified system	16
Figure 3-3.	VS-PSH response to load event during generating mode	17
Figure 3-4.	VS-PSH response to load event during generating mode (Cont.)	18
Figure 3-5.	VS-PSH response to load event during pumping mode	19
Figure 3-6.	VS-PSH response to load event during pumping mode (Cont.)	20
Figure 4-1.	T-PSH schematic during generating, pumping and HSC operating modes	22
Figure 4-2.	T-PSH system diagram	23
Figure 4-3.	T-PSH response to load event during generating mode	24
Figure 4-4.	T-PSH response to load event during generating mode (Cont.)	25
Figure 4-5.	T-PSH response to load event during pumping mode	26
Figure 4-6.	T-PSH response to load event during pumping mode (Cont.)	27
Figure 4-7.	T-PSH response to load event during HSC mode	28
Figure 4-8.	T-PSH response to load event during HSC mode (Cont.)	29
Figure 4-9.	T-PSH response to mode switching	31
Figure 4-10.	T-PSH response to mode switching (Cont.)	32

LIST OF TABLES

Table 0-1. Acronyms	8
Table 4-1. Steady-state T-PSH behavior results	23

NOMENCLATURE

Table 0-1. Acronyms

Abbreviation	Definition
PSH	Pumped Storage Hydropower
FS-PSH	Fixed-Speed Pumped Storage Hydropower
VS-PSH	Variable-Speed Pumped Storage Hydropower
T-PSH	Ternary Pumped Storage Hydropower
DFIG	Doubly-Fed Induction Generator
GSC	Grid-Side Converter
RSC	Rotor-Side Converter
DC	Direct Current
HSC	Hydraulic Short Circuit
p.u.	Per Unit
P_{Ref}	Active power setpoint
H	Head
K_D	Power distribution factor
P_{Mech}	Mechanical active power
P_{Out}	Overall active output power

1. INTRODUCTION

Pumped Storage Hydropower (PSH) is a mature hydro technology whose first use dates back to the 1890s. PSH plants' service to the grid is important in many aspects: they can provide frequency regulation, load leveling, black-start capabilities and increased generating capacity [1]. PSH plants can work either "open-loop", with a naturally flowing mass of water as a lower reservoir, or in "closed-loop" configuration in two independent reservoirs. According to [2], PSH plants accounted for a 93% of utility-scale energy storage in the United States (US) in 2021. All PSH plants can work in two basic different operating modes: either generating mode - providing active power - or pumping mode - absorbing active power.

The most common type of PSH is the Fixed-Speed (FS)-PSH: simple and widely employed, it can provide frequency regulation or spinning reserve in generating mode. All of the PSH plants in the US correspond to this type of technology [1]. More recently developed, the Variable-Speed (VS)-PSH extends the capabilities of FS-PSH thanks to power electronics. Although its initial cost is higher, VS-PSH can provide frequency regulation in both generating and pumping modes, its operation modes are more flexible, and the potential revenue is higher [3]. Finally, Ternary (T)-PSH units provide an even faster switching between generating and pumping modes, bringing more flexibility in case that it is needed.

Three different models: a FS-PSH, a VS-PSH and a T-PSH, have been developed for Simscape, the Simulink environment for developing physical systems. The goal of this report is to document and introduce the developed models, and to show their dynamic response to a load event. For simulation purposes, the FS-PSH and T-PSH models are integrated into the IEEE 39 bus system [4]. The system is modified to include the FS-PSH and T-PSH. However, due to the demanding computation requirements for the VS-PSH, it has been simulated in a simplified three-bus system.

The motivation for explaining and sharing these PSH models resides on the lack of PSH state-space models that are publicly available. The distribution of these models aim to fuel and inspire research on the PSH integration into the grid. The models are publicly available on this GitHub repository¹. If used, please cite this report².

¹ See: https://github.com/sandialabs/Simulink_PumpedStorageHydropower.

² M. Jimenez-Aparicio et al., "Simulink Modeling and Dynamic Study of Fixed-Speed, Variable-Speed, and Ternary Pumped Storage Hydropower," Sandia Technical Report, September 2022.

2. FIXED-SPEED PSH

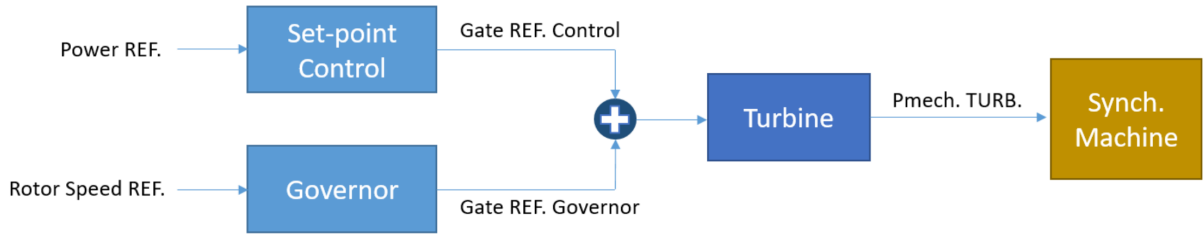
2.1. Model description

A Fixed-Speed (FS), or “conventional”, hydropower plant consists of a synchronous machine or an induction generator that works at synchronous speed. It is a mature and reliable technology, and the vast majority of PSH in the world are FS-PSH [5]. The cost is significantly lower than other more advanced (and more complex) PSH technologies. The model presented in this report is based on a synchronous machine. For this reason, it requires a governor for frequency regulation. The elements in the developed Simulink model are:

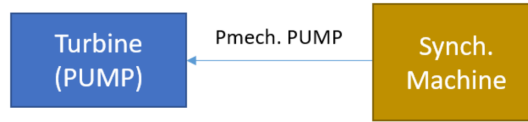
1. A setpoint control, which calculates the gate opening command based on the deviation between the actual output power and the selected power reference. The gate’s opening ranges between [0.05, 0.5] p.u. The setpoint control is only used during generating mode.
2. A governor, which further modifies the gate opening to correct the frequency deviation. The governor setpoint is added to the gate opening command previously calculated in the setpoint control. The governor is only used during generating mode, so frequency-droop control adjustments can be only observed in this operating mode.
3. A turbine model, used for generating mode simulations [6].
4. A voltage regulator and exciter, based on the IEEE type AC1A excitation system model.
5. A 3-phase, 125 MVA, 18 kV synchronous machine modeled in the D-Q rotor reference frame.

As a PSH, the hydropower plant works as a pump as well. However, the pumping mode doesn’t use any regulator or control. In pumping mode, the synchronous machine is set to work at nominal power. The fact that the pump is operating at constant load prevents the FS-PSH to provide frequency regulation or spinning reserve [7]. Regarding the output power constraints, a FS-PSH plant can typically operate in the range from 0.4 to 1 p.u. while in generating mode. For pumping mode, the lower limit is set to -1 p.u. [8]. The FS-PSH block structure is detailed in Fig. 2-1. Note that there is no control for the pumping mode.

The two use cases that are presented below show the model response to a load event (or load pulse), which corresponds to a 300 MW load being connected at $t = 130$ seconds, and being disconnected at $t = 220$ seconds. Both the FS-PSH model and the aforementioned load are located at bus 2 in the IEEE 39 bus system, as it can be observed in Fig. 2-2. Both generating and pumping modes for the FS-PSH are analyzed. The system is at steady state before the load connection.



(a) FS-PSH diagram in generating mode



(b) FS-PSH diagram in pumping mode

Figure 2-1. FS-PSH diagram

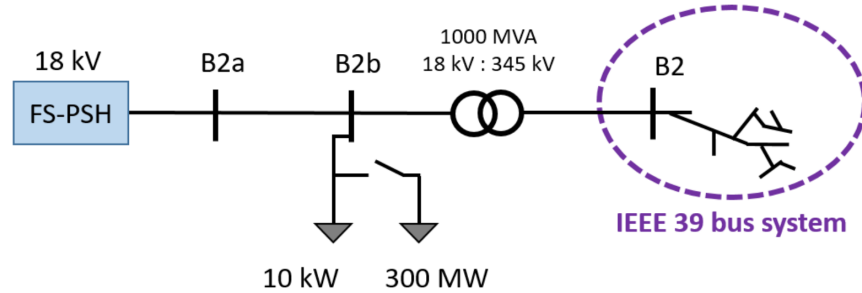


Figure 2-2. FS-PSH location in the IEEE 39 bus system

2.2. Simulation: Load event for the FS-PSH in generating mode

In this simulation, the power reference setpoint for generating mode is $P_{Ref} = 100$ MW, which matches the FS-PSH output power that can be observed in Fig. 2-3. The load event makes the governor to vary its output to cancel the frequency deviation, and a slight transient can be seen in the turbine gate opening. Eventually, this modifies the power output of the FS-PSH as well. A zoom in into the FS-PSH output active power dynamic around the setpoint at the time of the load connection is provided. However, neither the frequency-droop control nor the change in the FS-PSH output are as fast as other resources, and that is the reason why the magnitude of the response is relatively small. It is also noticeable the “opposite” reaction typically associated to hydro models at the start of the load pulse. This can be seen on the gate opening: the response to a load increase should be produce more power, which is the opposite of what actually happens in the beginning.

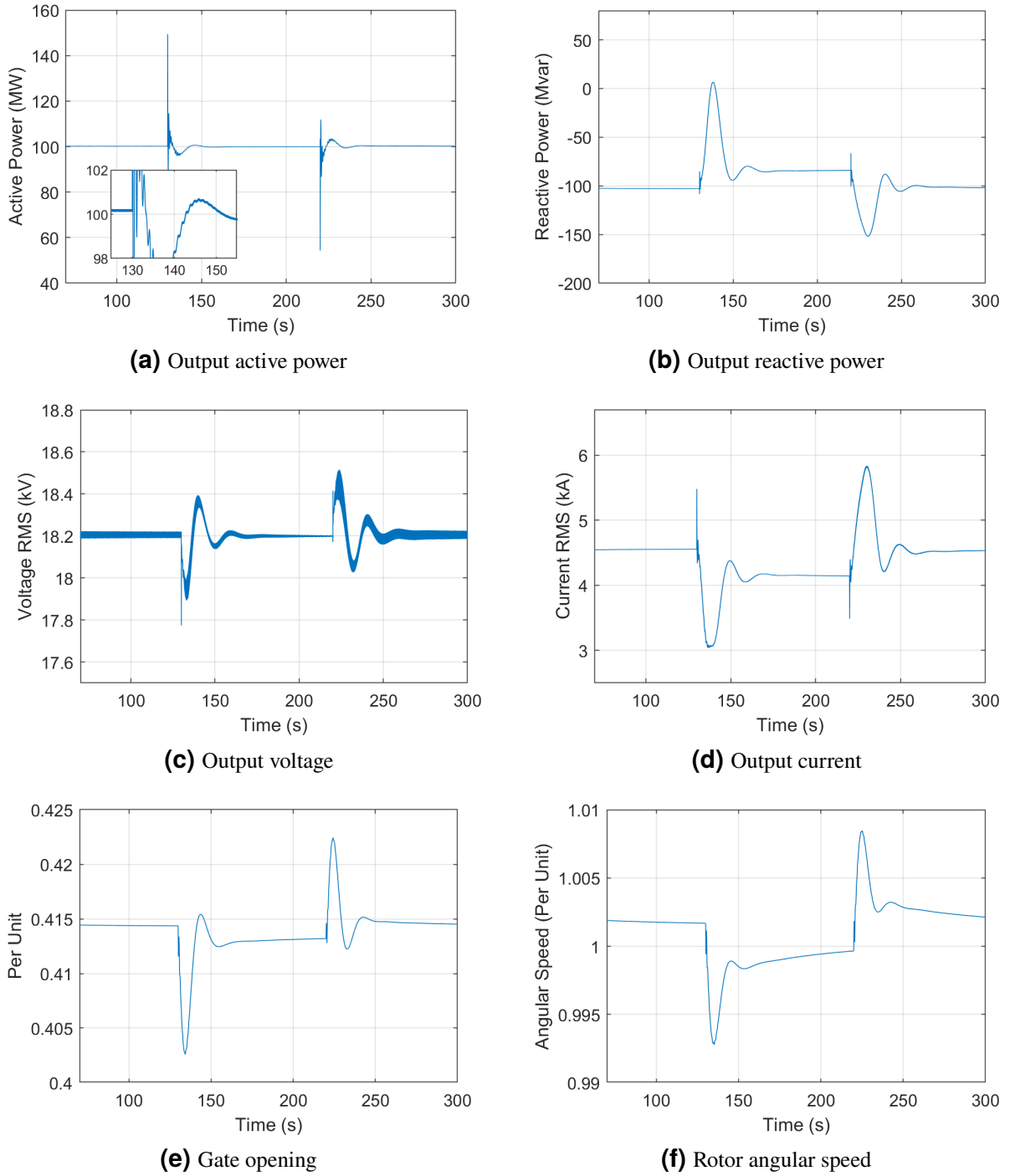


Figure 2-3. FS-PSH response to load event during generating mode

2.3. Simulation: Load event for the FS-PSH in pumping mode

As opposed to the generating mode, the FS-PSH only works at nominal power during pumping mode, which is equal to absorbing 125 MW as it can be seen in Fig. 2-4. The FS-PSH doesn't have any frequency-droop control or set-point control. The transient in the output active power is due to

changes in the mechanical speed, and it comes back to the reference shortly after the load pulse as the generation imbalance is addressed by other resources. In this mode, the gate opening (of the turbine) variable is not applicable, and therefore it is not shown.

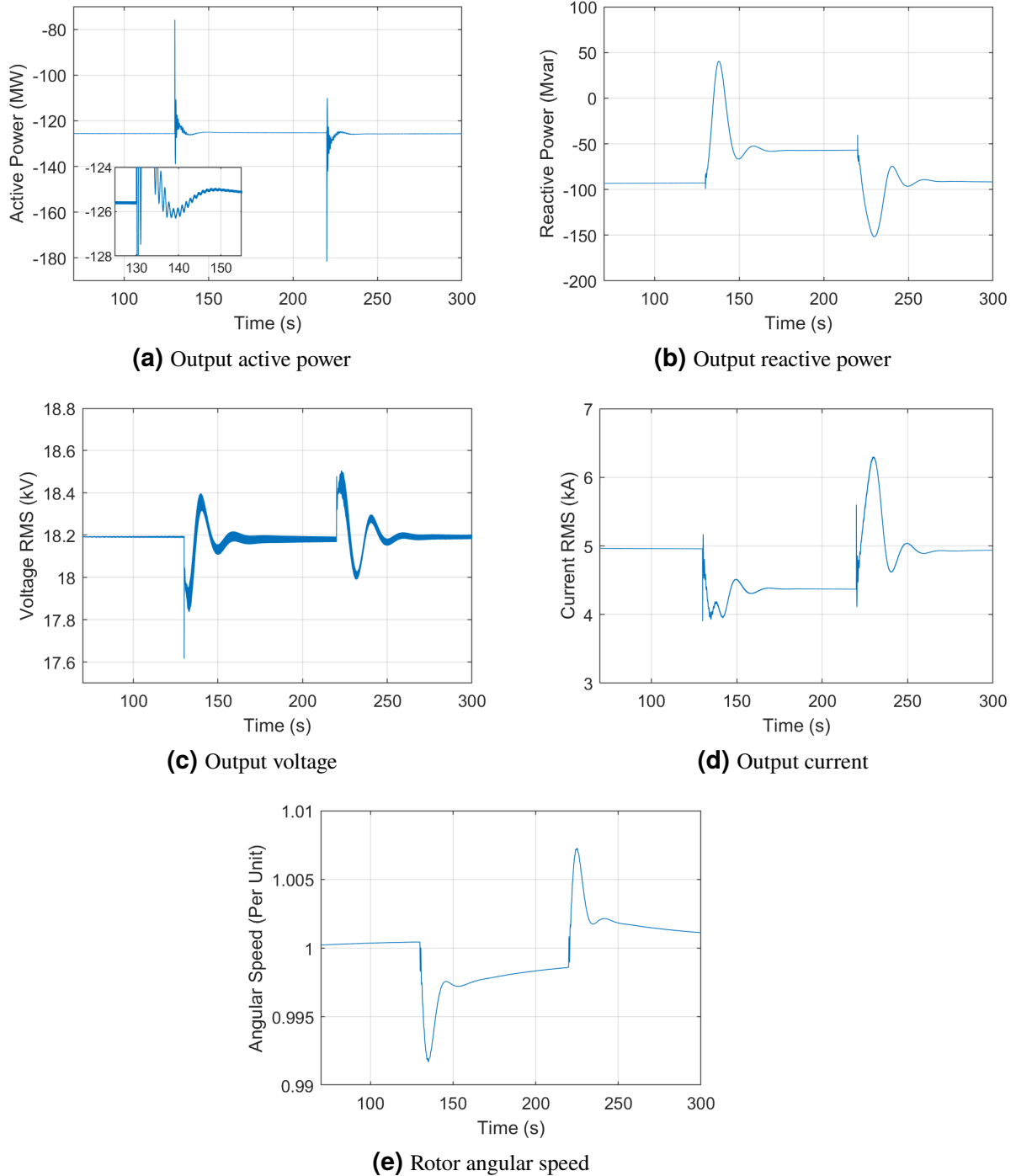


Figure 2-4. FS-PSH response to load event during pumping mode

3. VARIABLE-SPEED PSH

3.1. Model description

Variable-Speed (VS)-PSH, also known as “Adjustable-Speed” PSH, merges power electronics and a conventional hydro-power plant to deliver an increased flexibility in the operation with more relaxed output constraints. Similarly to the FS-PSH design, the VS-PSH output power constraints during generating mode range from 0.4 to 1 p.u., but VS-PSH pumping operation is increased from a single setpoint at nominal power to a broader operation from -0.7 to -1 p.u. [8]. This technology has been largely researched in Type III wind turbines since the 1990s [9, 10].

Some of the benefits of VS-PSH are their ability to provide grid stability and frequency regulation in any operating mode. This is still an emerging technology, and just a few plants of this type have been commissioned in the world [5]. From an economic point of view, VS-PSH can potentially increase the revenue compared to FS-PSH [7].

The type of induction machine known as Doubly-Fed Induction Generator (DFIG) is the current standard in VS-PSH. Generally speaking, a DFIG is a wound rotor induction machine that can be used at variable speed operation within a certain range of the synchronous speed [11]. This is achieved thanks to a back-to-back converter located in parallel to the induction generator. One side of the converter is connected to the grid, while the other side is connected to the rotor. The Rotor Side Converter (RSC) can inject current with varying frequencies in order to achieve the desired frequency in the stator [5]. The power is transferred to the grid in two different paths: On the one hand, the majority of the provided power is the DFIG stator output. On the other hand, some power is provided by the Grid-Side Converter (GSC). There is a trade-off between the stator output power and the total provided power, which implies a larger GSC contribution in order to achieve a larger output power. The direction and magnitude of the rotor power depends on the rotor angular speed, which eventually depend on the operating mode. A typical slip for a plant of this type is $\pm 10\%$, but it can go up to $\pm 30\%$ [5]. The rotor angular speed ω is optimized to achieve an efficient turbine operation, and it can be calculated with a linear relationship as detailed in (3.1):

$$\omega(P_{Ref}, H) = 1.25(P_{Ref} - 0.8) - 0.25(H - 0.8) - 0.05 \quad (3.1)$$

where P_{Ref} is the power setpoint and H is the head (the difference in height between the hydro intake and the discharge points) [12].

The VS-PSH model has the following elements:

- A 3-phase, 300 MVA, and 18 kV wound rotor induction generator, implemented as a DFIG.

- A GSC, implemented as an averaged model. The power injection/ extraction to the DC link is modeled as a current source.
- A RSC, following the same design as the GSC.
- A DC link, consisting of a large capacitor, which interfaces both the RSC and GSC.
- A gate optimizer block, which implements the expression in (3.1). The gates have an operating range between [0.075, 1.2] p.u., and a maximum speed of 0.1 p.u./second.
- A governor, which calculates the gate opening to achieve the requested power reference, and which provides frequency regulation in both generating and pumping modes.

The VS-PSH high-level diagram can be seen in Fig. 3-1.

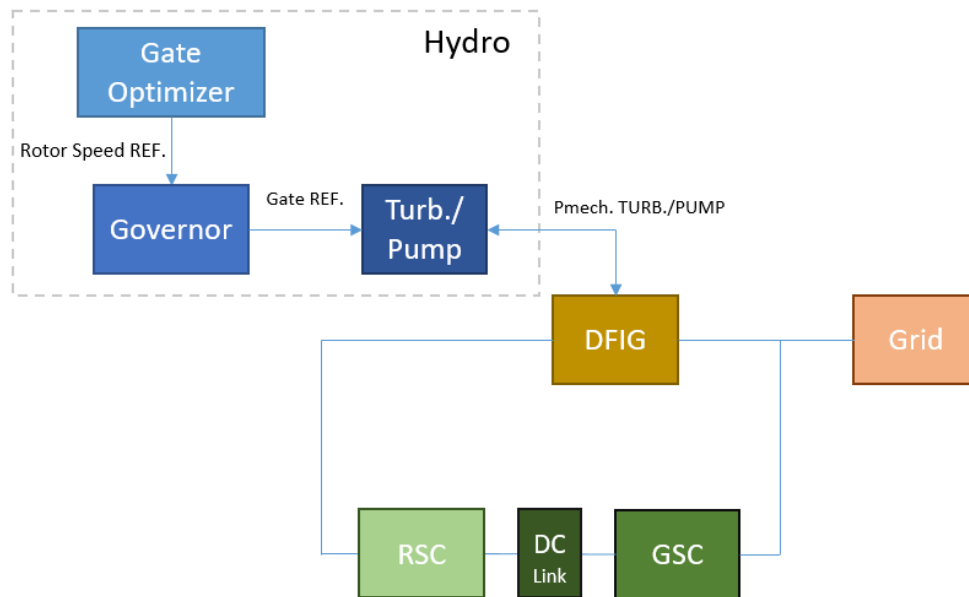


Figure 3-1. VS-PSH system diagram

The simulation of the VS-PSH requires a multi-step initialization process in which several key components are progressively turned on prior to reaching a steady state. The 5-step process is detailed as follows. The initialization is the same for both generating and pumping modes.

1. GSC initialization (at $t = 2$ seconds). The GSC and associated controls are fully turned on. The GSC control aims to maintain the DC link voltage at 40 kV, but the voltage is still artificially kept at that level by a voltage supply source. Therefore, the GSC is not actively regulating at this time and the output power is zero. The rotor angular speed is stable at 1 p.u., as it is controlled by an initialization control that aims to reach a predefined speed reference.
2. The voltage source that bypasses the DC link prior to this step, and keeps the voltage stable at 40 kV, is removed (at $t = 3$ seconds). At this moment, the GSC starts to regulate. The GSC output power is still zero because the DC link voltage is stable.

3. Partial initialization of RSC (at $t = 4$ seconds). The connection of the RSC with the DC link is established, but the RSC controls are still turned off.
4. Total initialization of RSC (at $t = 5$ seconds). The RSC controls are activated, and the rotor reference output current is controlled to deliver the required output power. The stator starts to generate or absorb power, and the rotor angular speed reference is now set at a 1.15 p.u. as the speed limits are updated. A transient to achieve such rotor speed begins.
5. The VS-PSH governor is turned on (at $t = 10$ seconds). The angular speed control is replaced by the governor, which takes into account the physical model of the hydro plant. The power electronics devices are fully engaged, and some power is either generated or drawn from the grid by the GSC. The steady state is finally achieved around $t = 30$ seconds.

The dynamics of developed model are tested on a simplified three-bus system, which is composed of the VS-PSH, a 50 MW load and an infinite voltage source, as shown in Fig. 3-2. To produce the load event, which is a 10 second load pulse, an extra load of 50 MW is switched on. The load event occurs once the system has been initialized, at $t = 35$ seconds, and it lasts until $t = 45$ seconds. As a disclaimer, this model is extremely expensive both in computing power and memory requirements. Just a fraction of all the variables can be saved for later analysis, and the total simulation time is limited. The test system has to be simplified for the same reason. In order to achieve stability in more complex systems, additional modifications of the controls or the interface may be required.

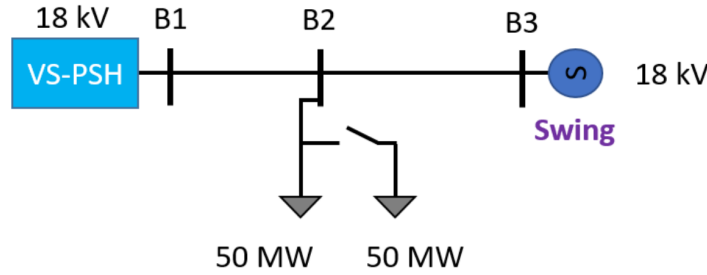


Figure 3-2. VS-PSH location in the simplified system

Two use cases are presented below: the load events during generating and pumping modes. The recorded variables are the VS-PSH outputs (active and reactive power, voltage and current), as well as the DFIG stator and GSC active and reactive power in order to visualize the operation of the plant. However, in this work, the voltage source unfortunately hides most of the dynamics.

3.2. Simulation: Load event for the VS-PSH during generating mode

During generating mode, the VS-PSH outputs a total of 235 MW. Although $P_{Ref} = 1$, the optimizer in (3.1) determines a lower power setpoint (around 0.7 p.u.). Most of the active power comes from

the stator, approximately 210 MW, and the remaining 25 MW comes from the GSC. The rotor speed is around 1.14 p.u., and the output reactive power is oscillating around 0 Mvar. The GSC effectively maintains the DC link voltage around 40 kV. The transients during the load event are small because of the low system inertia (the infinite voltage source handles most of the perturbation), but it can be appreciated how there is an effect on the VS-PSH behavior.

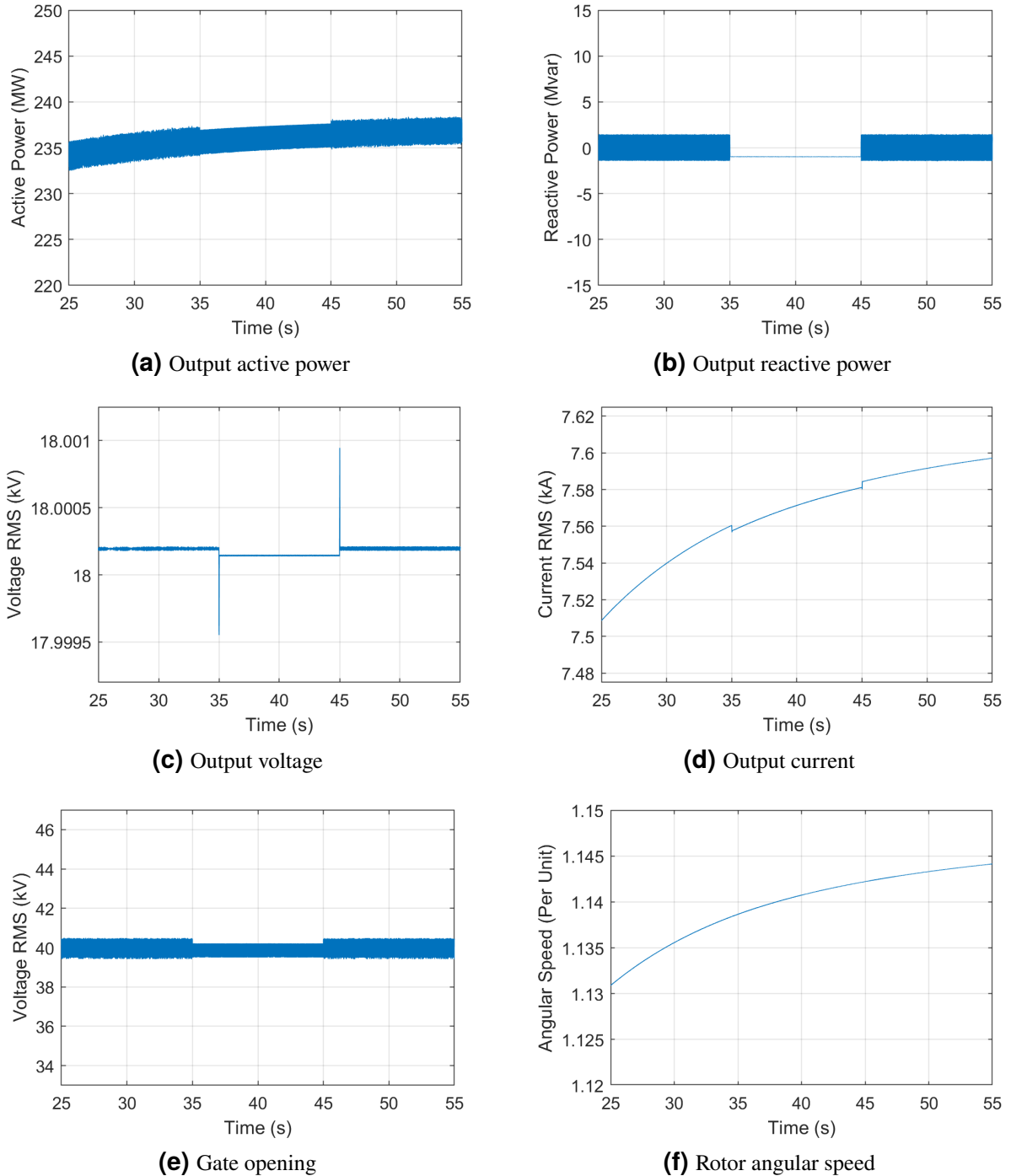


Figure 3-3. VS-PSH response to load event during generating mode

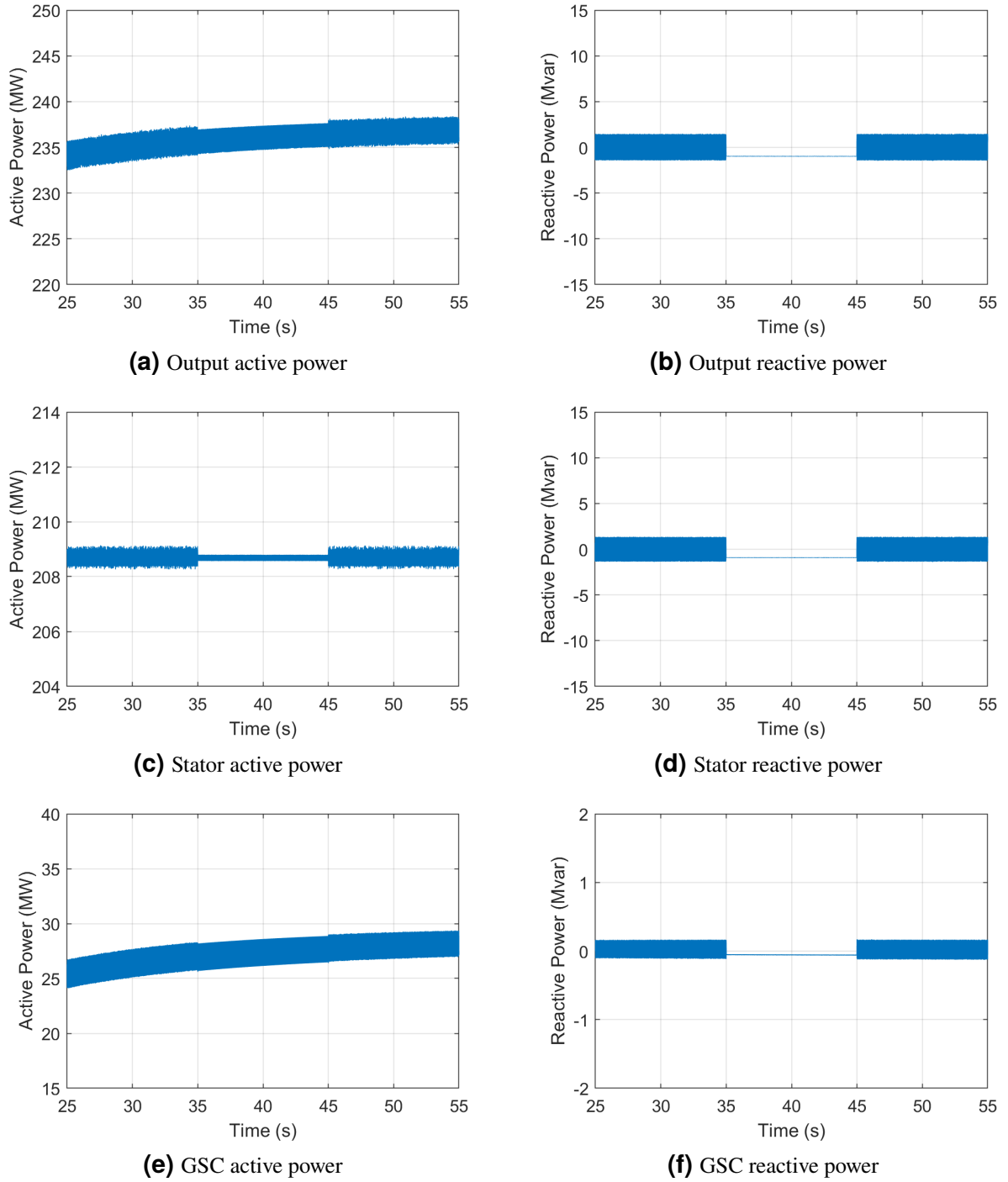
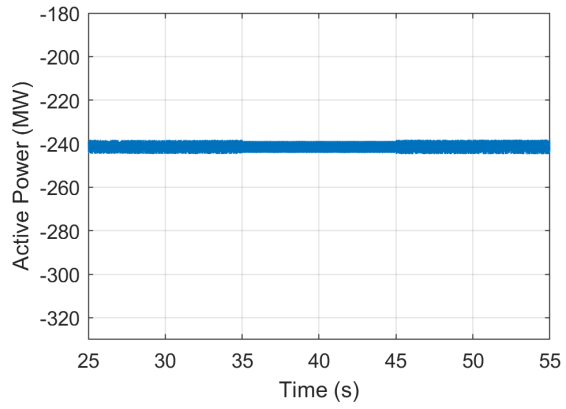


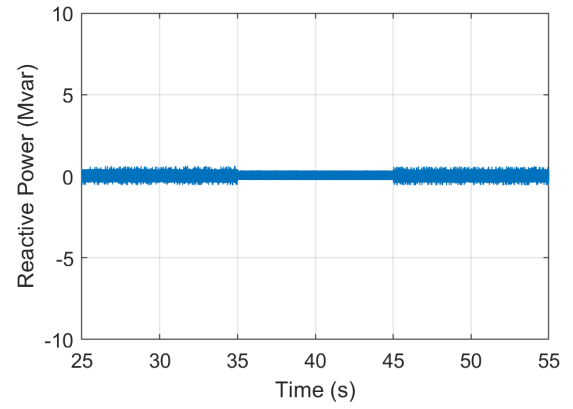
Figure 3-4. VS-PSH response to load event during generating mode (Cont.)

3.3. Simulation: Load event for the VS-PSH during pumping mode

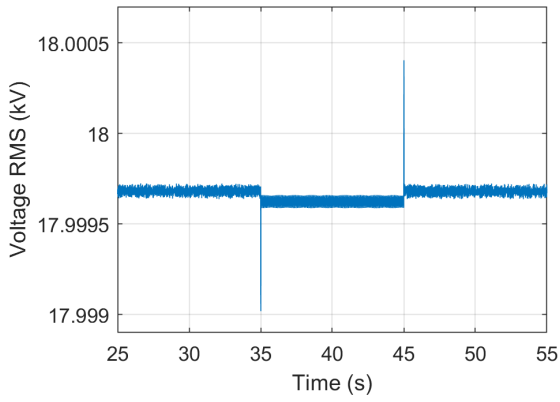
The dynamics are similar to the generating mode. This time, the VS-PSH is absorbing power. In particular, the GSC absorbs around 35 MW, while the DFIG stator absorbs between 205 to 210 MW. This gives a total of 240 MW absorbed by the VS-PSH as a whole.



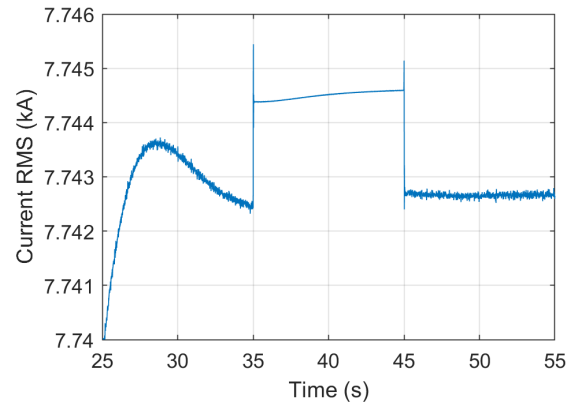
(a) Output active power



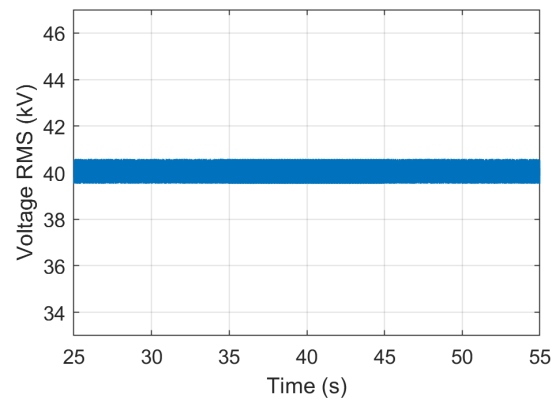
(b) Output reactive power



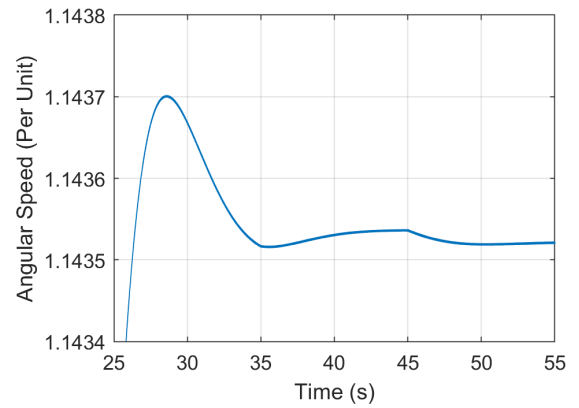
(c) Output voltage



(d) Output current

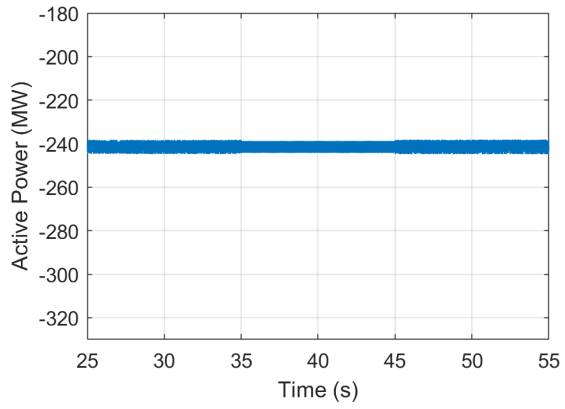


(e) DC link voltage

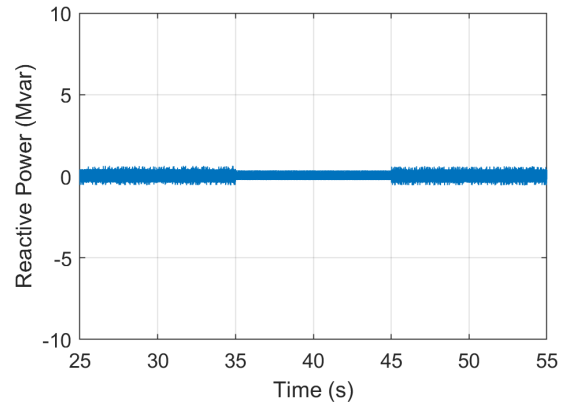


(f) Rotor angular speed

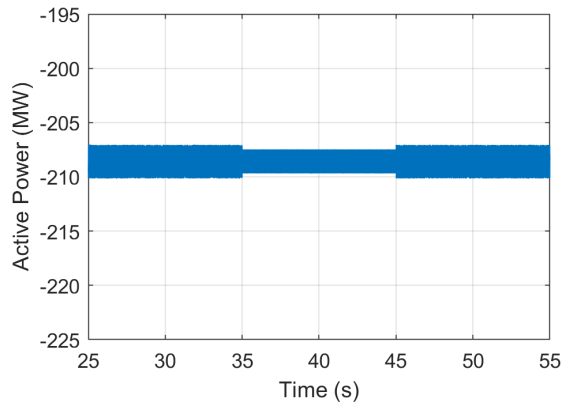
Figure 3-5. VS-PSH response to load event during pumping mode



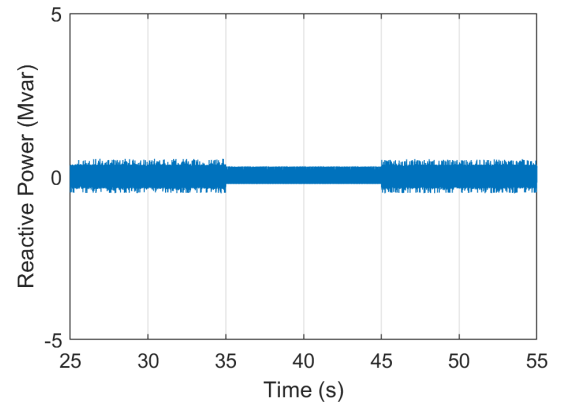
(a) Output active power



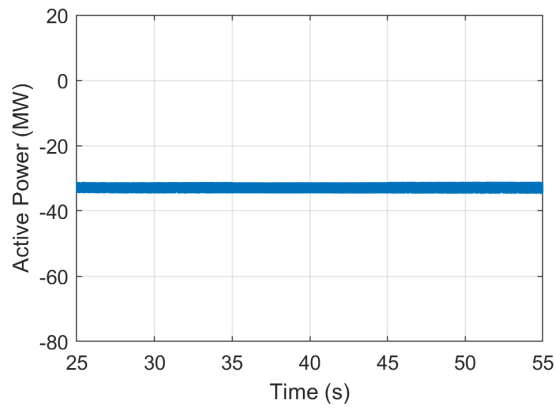
(b) Output reactive power



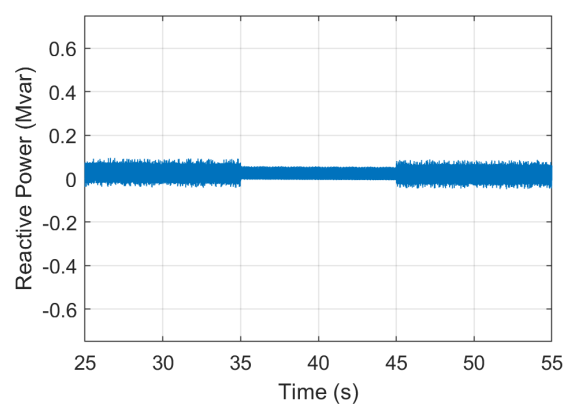
(c) Stator active power



(d) Stator reactive power



(e) GSC active power



(f) GSC reactive power

Figure 3-6. VS-PSH response to load event during pumping mode (Cont.)

4. TERNARY-PSH

4.1. Model description

T-PSH plants are equipped with separated turbine and pump units. Both elements have rotating shafts aligned on the same axis, which is connected by a clutch. Depending on the operating mode, the turbine, the pump and their respective valves may be active or not. The schematics for each mode can be observed in Figure 4-1. During generating mode, only the clutch C1 is engaged to transfer mechanical power to the generator. The turbine valve is open, while the pump valve is closed. On the contrary, only clutch C2 is engaged during pumping mode. The pump valve is open while the turbine valve is closed. Finally, during Hydraulic Short Circuit (HSC) mode both clutches C1 and C2 are engaged, both turbine and pump valves are open, and the shared axis spins at the same angular speed [13].

As the axis always spins in the same direction, the change from one mode to another takes just a few seconds. It mainly depends on the action of the clutches and the valves. In [14], the required time for switching between generating and pumping modes in the T-PSH is compared to those in the FS and VS-PSH plants. The results show that T-PSH is by far the fastest technology. The mode switching in the T-PSH model is analyzed later as a separate experiment.

However, a standard T-PSH unit would only provide frequency regulation in generating mode (it essentially resembles a FS-PSH) [1]. In order to provide frequency regulation while pumping, there is a third operating mode, HSC mode, in which both the turbine and pump work in a closed loop. The pump absorbs more energy than what the turbine can produce so, overall, the T-PSH has a certain pumping behavior during HSC mode [6].

Another advantage of the T-PSH is that this technology also offers an increased flexibility in the power setpoint in both generating and pumping modes. Any power reference from 0.3 p.u. to 1 p.u. (in generating mode), -1 p.u. (pumping mode) or from -0.6 p.u. to 0 p.u. (in HSC mode) can be achieved [8].

The elements in the T-PSH model, which can be observed in Fig. 4-2, are:

1. A power distribution block, which calculates the turbine and pump power setpoints depending on the operating mode. These setpoints vary over time in the “mode switching” experiment. The flags that manage the switching between transfer functions are calculated here as well.
2. A governor, which calculates the turbine and pump gate opening. In pumping case, this is just a simple arithmetic operation. During a generating case, the turbine gate reference is represented by a transfer function. In addition, this gate reference is sensitive to frequency variations during the generating mode.

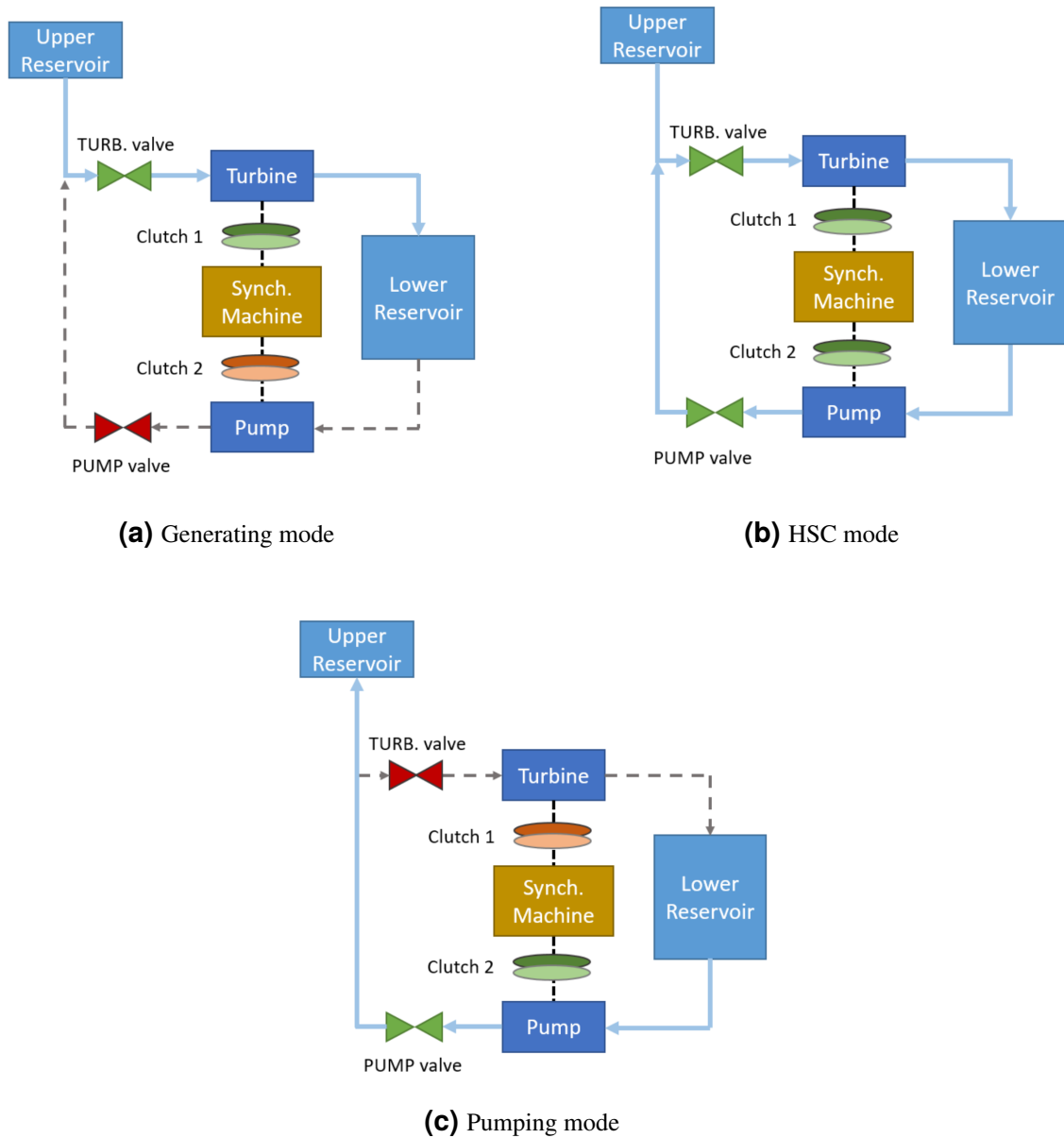


Figure 4-1. T-PSH schematic during generating, pumping and HSC operating modes

3. A pump and turbine gate models, which have an operating range between $[0, 1]$ p.u., and a maximum gate opening/closing speed of 0.05 p.u./second.
4. Identical turbine and pump models [14]. There is a flag that determines if the penstock is shared or not in the head to flow conversion matrix. The combined output of the turbine and the pump is the generator's mechanical input.
5. A voltage regulator and exciter, based on the IEEE type AC1A excitation system model.
6. A 3-phase, 320 MVA, 18 kV synchronous machine modeled in the D-Q rotor reference frame.

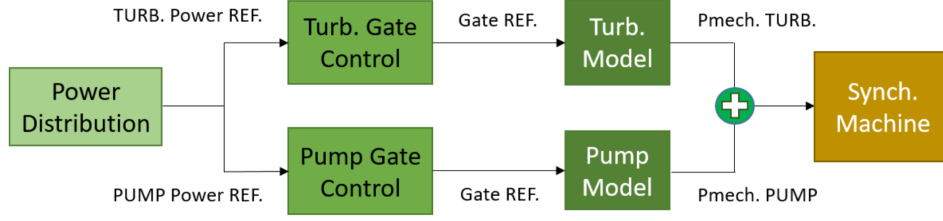


Figure 4-2. T-PSH system diagram

It is important to note that the mode switching experiment in a state-space based simulator, such as Simulink, requires considering all the different modes at the same time. For this reason, several transfer functions are defined in the model, and each one of them represents the corresponding operating mode. When a mode switch occurs, the new mode's transfer function must be reinitialized.

4.2. Simulation: Steady-state

For the T-PSH, the analysis of the steady-state becomes relevant to understand the plant's behavior in different modes. In Table 4-1, the distribution factor K_D , the mechanical power P_{Mech} for both turbine and pump, and the overall T-PSH output power P_{Out} are shown for each of the three considered operating modes. All quantities are in p.u., and K_D is in the range of [0, 1].

Table 4-1. Steady-state T-PSH behavior results

Mode	K_D Turbine	K_D Pump	P_{Mech} Turbine	P_{Mech} Pump	P_{Out}
Generating	1	0	0.8	0	0.8
Pumping	0	1	0	-0.9	-0.9
HSC	0.4	0.6	0.34	-0.54	-0.2

During HSC mode, the system works in a closed-loop where the turbine and pump are both working. The system is inherently lossy and, therefore, the amount of power absorbed by the pump from the grid is larger than the power generated by the turbine. This explains the slight pumping behavior of the T-PSH during HSC mode.

4.3. Simulation: Load Event

The dynamics of developed model are tested on the custom IEEE 39 bus system. To produce the power imbalance event, a load of 300 MW is connected to the system. The load is connected in the same bus as the T-PSH plant. The set-up for this experiment is identical as the one depicted in

Fig. 2-2. The load event occurs once the system has been fully initialized, at $t = 130$ seconds, and it lasts until $t = 220$ seconds.

As can be seen in Figs. 4-3, 4-4, 4-7 and 4-8, the T-PSH has frequency regulation only during the generating and the HSC modes. The turbine gate value increases due to the governor action, which increases the amount of mechanical power provided by the turbine, and eventually leads to an increase of the overall active power provided by the T-PSH. In the generating mode, the overall reactive power output remains fairly constant after an initial transient, although for the HSC mode it does change. Both the pump gate value and the pump mechanical power remain constant as there is no frequency-droop control in that element. Looking at the T-PSH current output it is possible to see that it increases due to the load event during the generating mode, which is the expected behavior. However, during the HSC mode, the current magnitude decreases instead. The reason for this behavior is that the T-PSH is working as a pump, but when the power increase is needed, its behavior starts to be closer to a turbine. Therefore, the amount of absorbed current decreases.

For the case of the pumping mode, the T-PSH doesn't provide any frequency regulation capabilities. The pump, which is the main element that is engaged in this period, doesn't have a frequency droop control. For the turbine, it is disabled in this operating mode. As it is shown in Figs. 4-5 and 4-6, both pump and turbine gate values are constant.

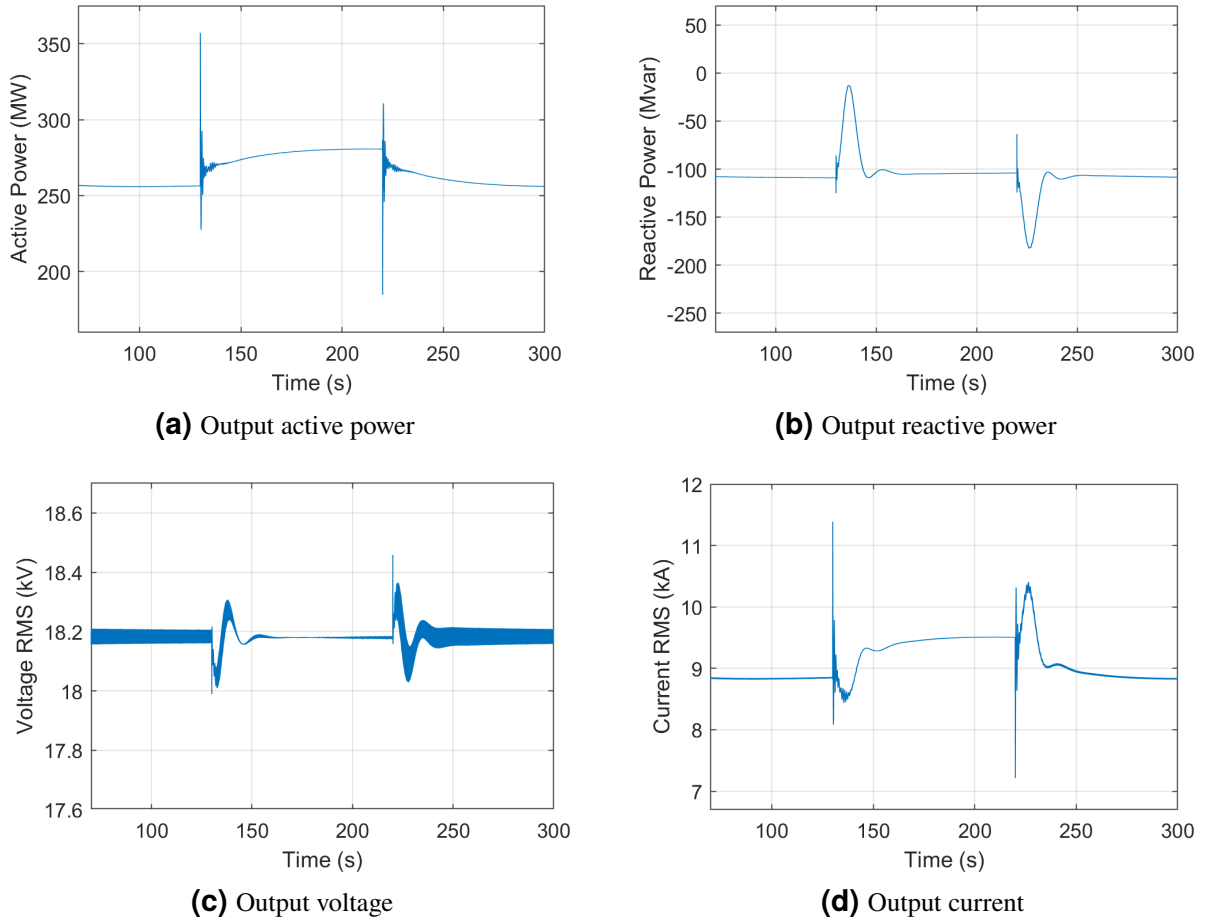
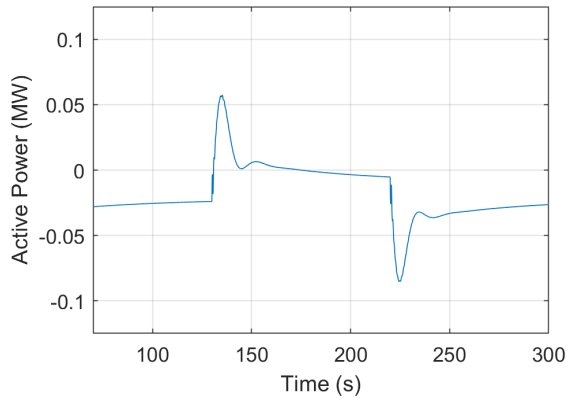
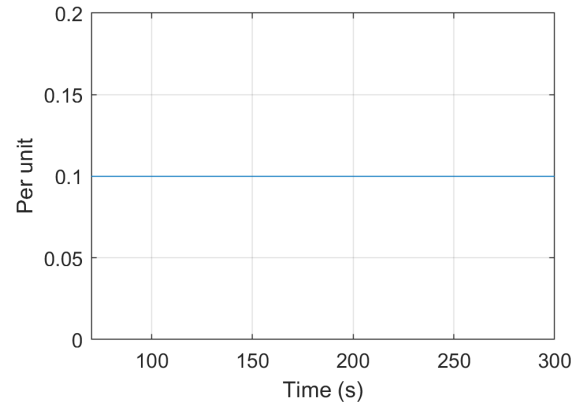


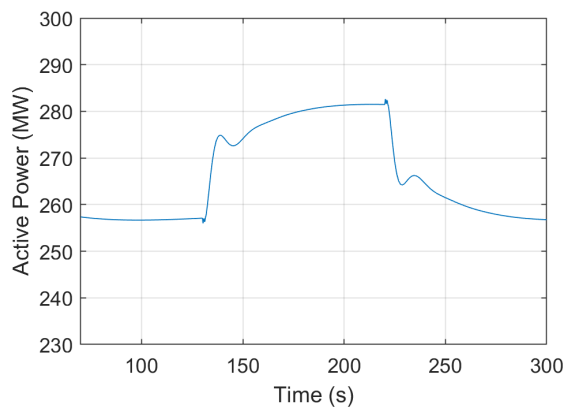
Figure 4-3. T-PSH response to load event during generating mode



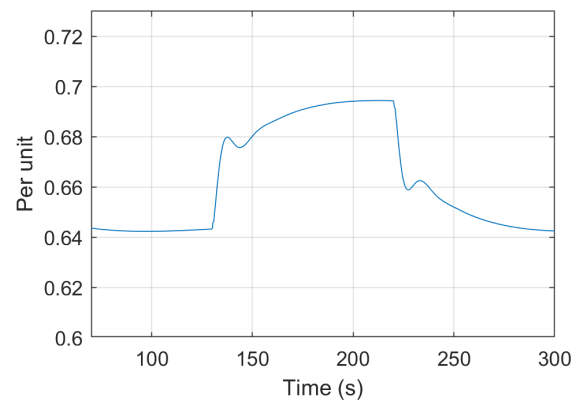
(a) Pump mechanical power



(b) Pump gate value

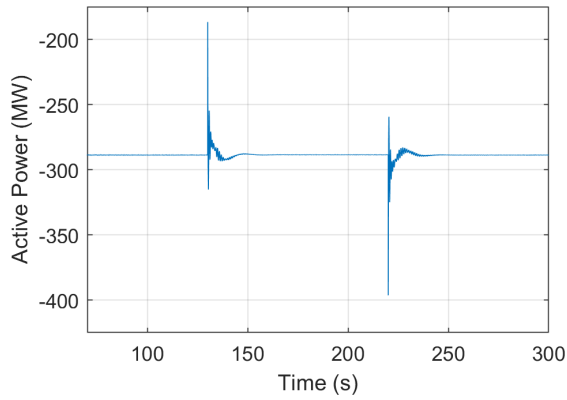


(c) Turbine mechanical power

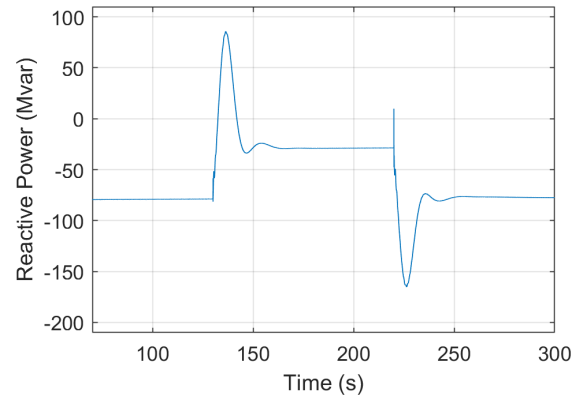


(d) Turbine gate value

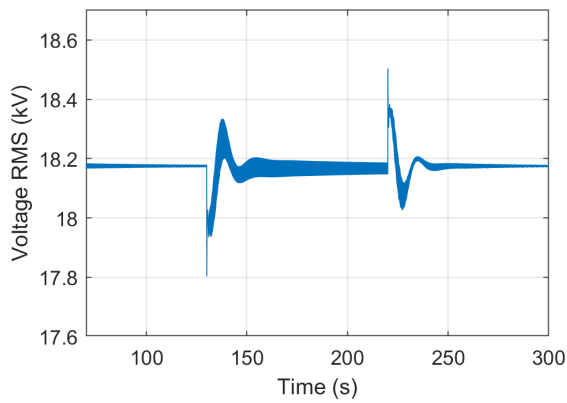
Figure 4-4. T-PSH response to load event during generating mode (Cont.)



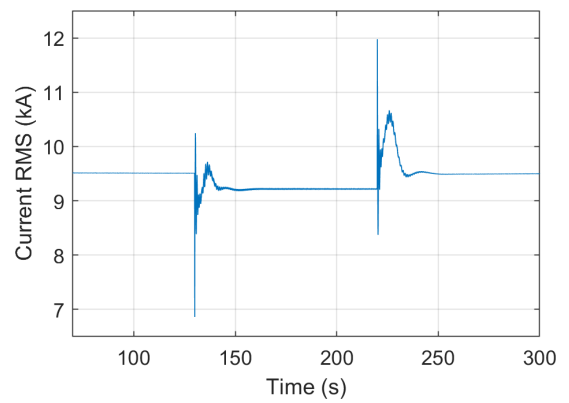
(a) Output active power



(b) Output reactive power

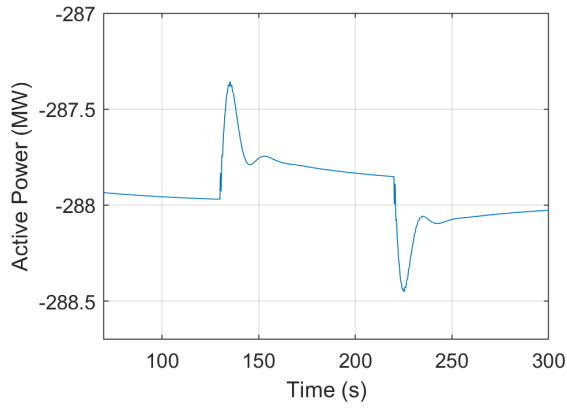


(c) Output voltage

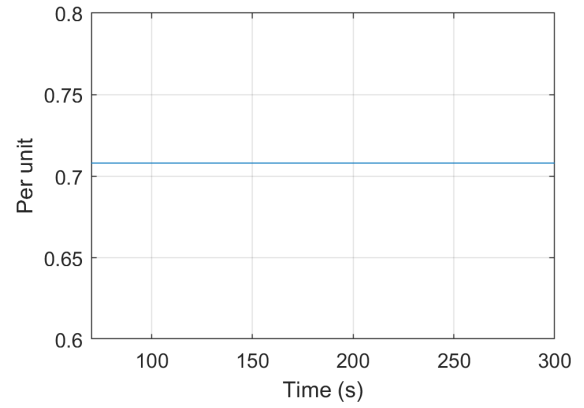


(d) Output current

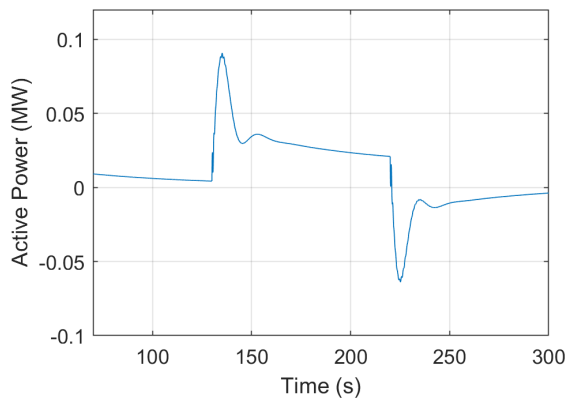
Figure 4-5. T-PSH response to load event during pumping mode



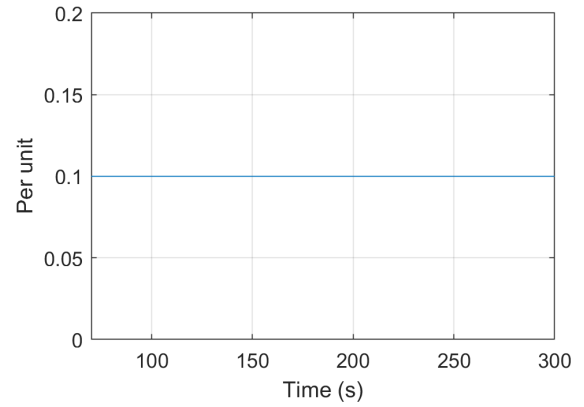
(a) Pump mechanical power



(b) Pump gate value

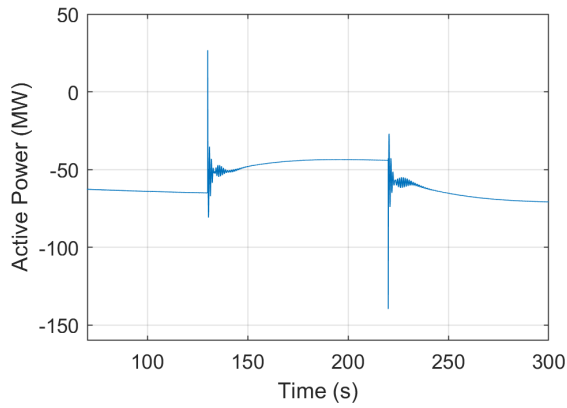


(c) Turbine mechanical power

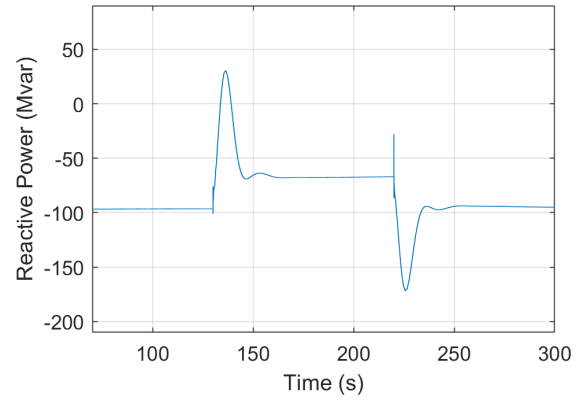


(d) Turbine gate value

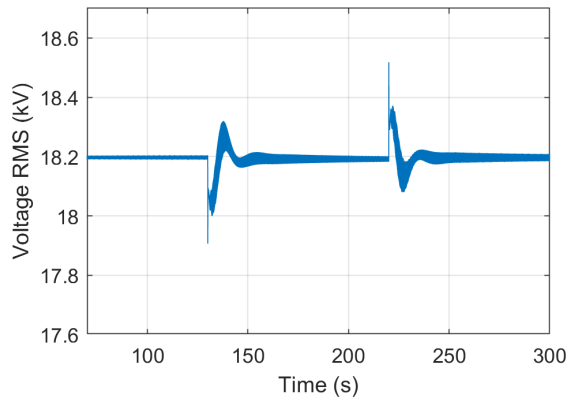
Figure 4-6. T-PSH response to load event during pumping mode (Cont.)



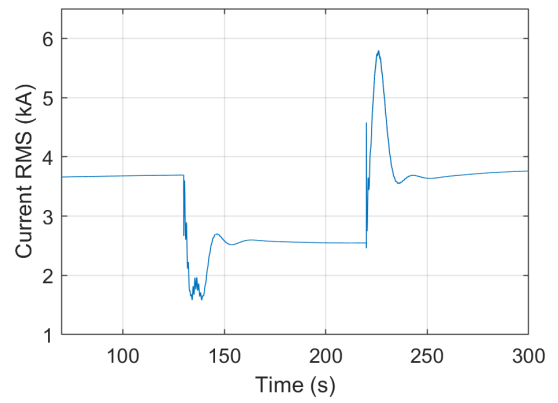
(a) Output active power



(b) Output reactive power

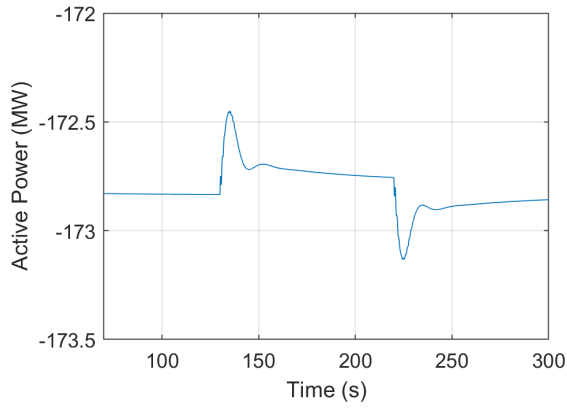


(c) Output voltage

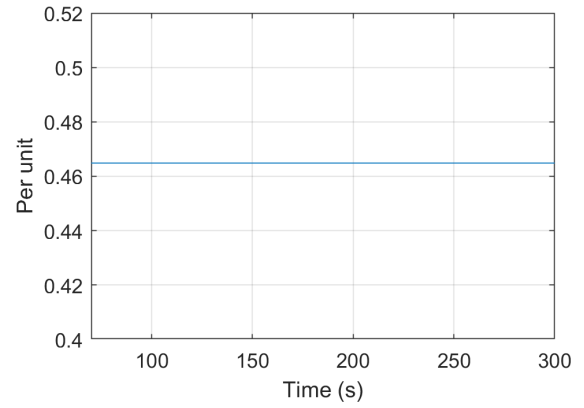


(d) Output current

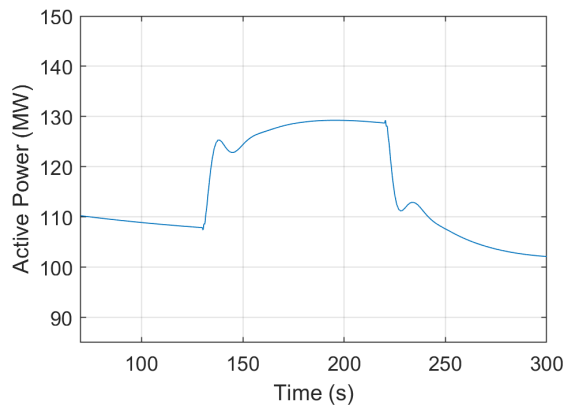
Figure 4-7. T-PSH response to load event during HSC mode



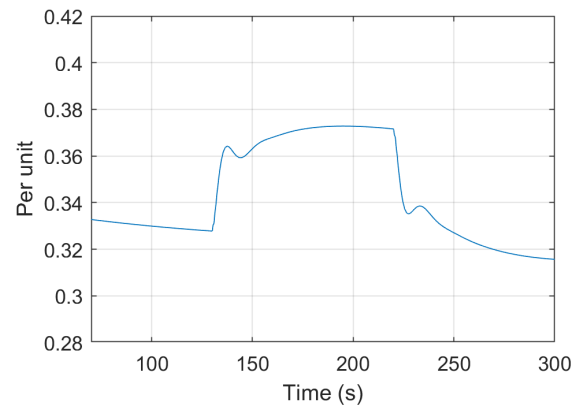
(a) Pump mechanical power



(b) Pump gate value



(c) Turbine mechanical power



(d) Turbine gate value

Figure 4-8. T-PSH response to load event during HSC mode (Cont.)

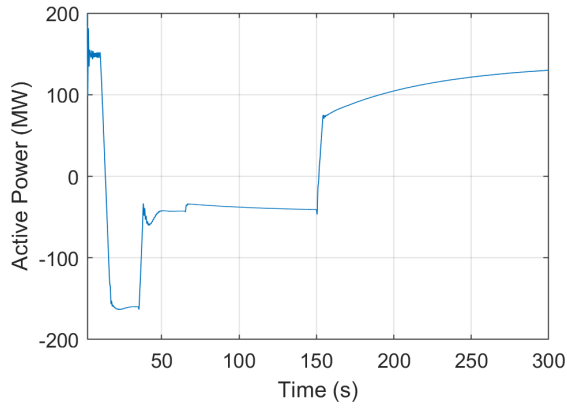
4.4. Simulation: Mode switching

The “mode switching” experiment shows the T-PSH behavior during three different events:

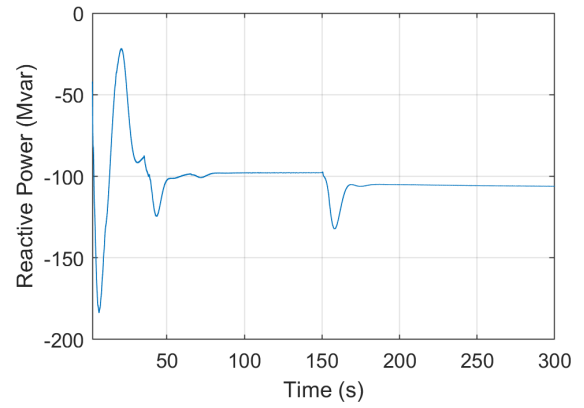
1. Generating mode to Pumping mode (at $t = 10$ seconds).
2. Pumping mode to HSC mode (at $t = 35$ seconds).
3. HSC mode to Generating mode (at $t = 150$ seconds).

Results are shown in Figs. 4-9 and 4-10. Regarding changes in the pump, they always occur at maximum speed. The pump governor changes its output immediately when a mode switch occurs. However, the gate opening is adjusted according to its speed limit. For the turbine, its governor is not as fast. According to [14], not all mode switchings occur at the same speed. The switching between generating to pumping mode occurs at maximum speed, as it just depends on the action of the valve. The situation is similar to change between pumping to HSC. However, the change from HSC to generating is remarkably slower. In Simulink, this is modeled in the following way: for fast transients (generating to pumping, and pumping to HSC), the turbine governor is just the static gain of the transfer function. Then, the setpoint change is immediate and the overall dynamics just depend on the gate velocity. Afterwards, once the switching is over, the steady-state transfer function kicks in to model the dynamic behavior of the plant. The transfer function is reinitialized to start directly on steady-state. On the other hand, for slow transients (such as HSC to generating), the entire transfer function is employed. For this experiment, $P_{Ref} = 0.5$ is employed. The HSC operating mode can be clearly observed as an operating mode between generating and pumping, but more leaned towards the last one.

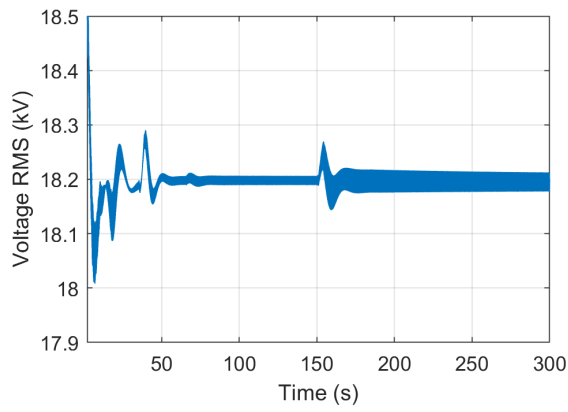
As for the switching times, the model is well aligned with [14]. The first switch (Generating mode to Pumping mode) is performed in about 10 seconds. The second switch (Pumping mode to HSC mode) takes around 30 seconds. Finally, the third switch is approximately in the new setpoint in around 100 seconds, although the turbine is still slowly moving towards the new steady state.



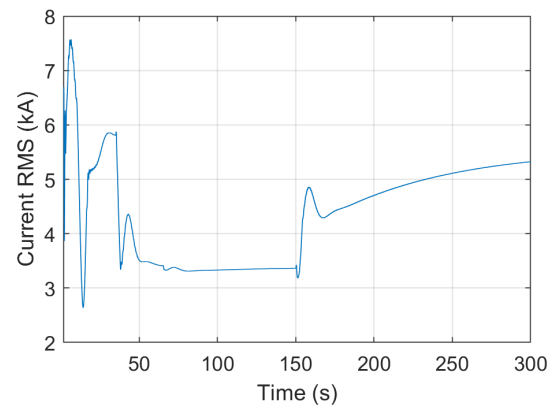
(a) Output active power



(b) Output reactive power

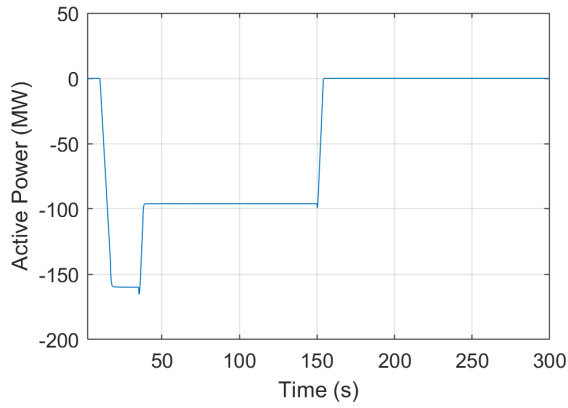


(c) Output voltage

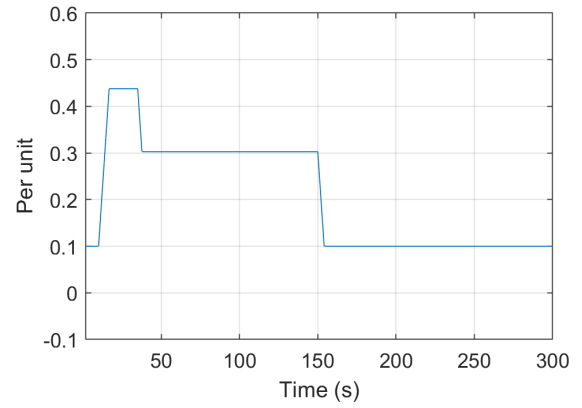


(d) Output current

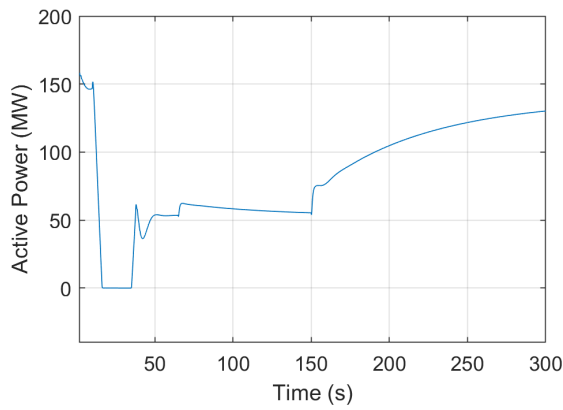
Figure 4-9. T-PSH response to mode switching



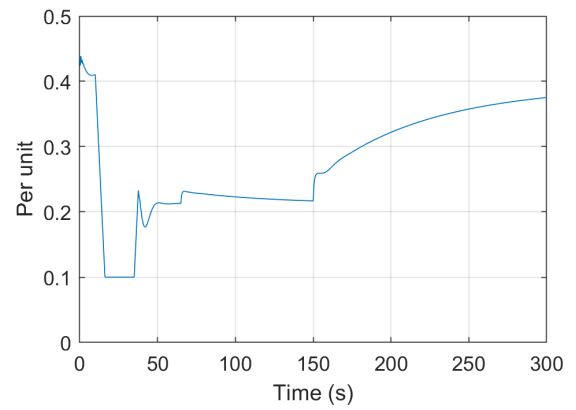
(a) Pump mechanical power



(b) Pump gate value



(c) Turbine mechanical power



(d) Turbine gate value

Figure 4-10. T-PSH response to mode switching (Cont.)

5. CONCLUSIONS

This report introduces three Pumped Storage Hydropower technologies models: Fixed-Speed (FS), Variable-Speed (VS) and Ternary (T). The models are developed in Simulink, and they are publicly available on this repository¹. Please, cite this report² if the models are employed.

An introductory description and the dynamic analysis for a load event of these models are presented. The output of each model matches their expected behavior. The FS-PSH achieves frequency regulation during generating mode only, although the effect of the frequency-droop control on the overall response is light. The VS-PSH, on the other hand, achieves frequency regulation during both generating and pumping modes thanks to the rotor speed regulation with power electronics. The operating range is increased in relation to FS-PSH in both generating and pumping modes. Finally, the T-PSH also achieves frequency regulation during generating and Hydraulic Short Circuit modes thanks to its design and the action of the clutches. For this technology, there is a total flexibility in generating and pumping operating modes. In addition, for the T-PSH, the steady-state, and the behavior during mode switching are also analyzed. The model correctly includes the fast switching speed among some of the operating modes.

¹ See: https://github.com/sandialabs/Simulink_PumpedStorageHydropower.

² M. Jimenez-Aparicio et al., “Simulink Modeling and Dynamic Study of Fixed-Speed, Variable-Speed, and Ternary Pumped Storage Hydropower,” Sandia Technical Report, September 2022.

BIBLIOGRAPHY

- [1] A. Botterud, T. Levin, and V. Koritarov, “Pumped Storage Hydropower: Benefits for Grid Reliability and Integration of Variable Renewable Energy,”
- [2] R. U. Martinez, M. M. Johnson, and R. Shan, “U.S. Hydropower Market Report (January 2021 edition),”
- [3] K. Mongird, V. Viswanathan, J. Alam, C. Vartanian, and V. Sprenkle, “2020 Grid Energy Storage Technology Cost and Performance Assessment,” tech. rep., 2020.
- [4] Y. Zuo, F. Sossan, M. Bozorg, and M. Paolone, “Dispatch and Primary Frequency Control with Electrochemical Storage: a System-wise Verification,” 2018.
- [5] E. Muljadi, R. M. Nelms, E. Chartan, R. Robichaud, L. George, and H. Obermeyer, “Electrical Systems of Pumped Storage Hydropower Plants: Electrical Generation, Machines, Power Electronics, and Power Systems,”
- [6] Siemens Power Technology, “PSSE Dynamic Simulation Models for Different Types of Advanced Pumped Storage Hydropower Units,” tech. rep., 2013.
- [7] A. Vargas-Serrano, A. Hamann, S. Hedtke, C. M. Franck, and G. Hug, “Economic benefit analysis of retrofitting a fixed-speed pumped storage hydropower plant with an adjustable-speed machine,” in *2017 IEEE Manchester PowerTech*, pp. 1–6, 2017.
- [8] S. Nag and K. Y. Lee, “Network and Reserve Constrained Economic Analysis of Conventional, Adjustable-Speed and Ternary Pumped-Storage Hydropower,” *Energies*, vol. 13, no. 16, 2020.
- [9] V. Gevorgian, S. Shah, W. Yan, and G. Henderson, “Grid-Forming Wind: Getting ready for prime time, with or without inverters,” *IEEE Electrification Magazine*, vol. 10, pp. 52–64, mar 2022.
- [10] S. Shah and V. Gevorgian, “Control, Operation, and Stability Characteristics of Grid-Forming Type III Wind Turbines: Preprint,”
- [11] S. Muller, M. Deicke, and R. De Doncker, “Doubly fed induction generator systems for wind turbines,” *Industry Applications Magazine, IEEE*, vol. 8, pp. 26–33, jun 2002.
- [12] E. Muljadi, M. Singh, V. Gevorgian, M. Mohanpurkar, R. Hovsapien, and V. Koritarov, “Dynamic modeling of adjustable-speed pumped storage hydropower plant,” in *2015 IEEE Power Energy Society General Meeting*, pp. 1–5, 2015.
- [13] J. W. Feltes, Y. Kazachkov, B. Gong, B. Trouille, P. J. Donalek, V. Koritarov, L. B. Guzowski, V. Gevorgian, S. Pti, and M. Americas, “Modeling Ternary Pumped Storage Units,” 2013.

- [14] Z. Dong, *Dynamic Model Development and System Study of Ternary Pumped Storage Hydropower*. PhD thesis, apr 2019.

DISTRIBUTION

Hardcopy—External

Number of Copies	Name(s)	Company Name and Company Mailing Address

Hardcopy—Internal

Number of Copies	Name	Org.	Mailstop

Email—Internal (encrypt for OUO)

Name	Org.	Sandia Email Address
Technical Library	1911	sanddocs@sandia.gov



Sandia
National
Laboratories

Sandia National Laboratories is a
multimission laboratory managed
and operated by National
Technology & Engineering
Solutions of Sandia LLC, a wholly
owned subsidiary of Honeywell
International Inc., for the U.S.
Department of Energy's National
Nuclear Security Administration
under contract DE-NA0003525.